Dependence of transient performance on potential distribution in a static induction thyristor channel*

Liu Chunjuan(刘春娟)†, Liu Su(刘肃), and Bai Yajie(白雅洁)

Institute of Microelectronics, School of Physical Science and Technology, Lanzhou University, Lanzhou 730000, China

Abstract: The impact of potential barrier distribution on the transient performance of a static induction thyristor (SITH) in a channel determined by geometrical parameters and applied bias voltage is studied theoretically and experimentally. The analytical expressions of potential barrier height and the I–V characteristics of the SITH are also derived. The main factors that influence the transient performance of the SITH between the blocking and conducting states, as well as the mechanism underlying the transient process, is thoroughly investigated. This is useful in designing, fabricating, optimizing and applying SITHs properly.

Key words: static induction thyristor; potential barrier; transient performance; blocking state; conducting state

DOI: 10.1088/1674-4926/33/4/044009 **PACC:** 6855; 7340Q; 7340T **EEACC:** 2550; 2560R

1. Introduction

Static induction thyristors (SITHs) have many excellent features, such as definitive conducting and blocking states, low conducting voltage-drop, high switching velocity, high current intensity, high voltage resistance, large power capability and high conversion efficiency. In recent years, scientists have paid great attention to SITHs. They are mainly interested in steady performance, such as the basic operating mechanism, the I–V characteristics and critical fabrication technologies[1−3]. However, SITHs are mainly used in large power switching application regions[4, 5]. The switching state means a transient process from one steady state to another. The switching on and switching off of a SITH is controlled by the potential barrier in the channel established by the static induction effects of gate and anode voltages[6−8]. So as a power switching device, the potential distribution in the channel of a SITH is an important parameter, by which the conducting voltage drop and blocking voltage is determined.

SITHs can block high voltages with a very small leakage current in the blocking state, and can conduct large current with a very small voltage drop in the conducting state. The channel is occupied entirely by the depletion layers of the gate-channel pn junctions in the blocking state. The increase in anode voltage the pn junction between the gate and drift region is reversely biased and the depletion layer mostly bears negatively biased voltage. In the conducting state, the electron and hole plasma established in the channel and drift regions results in a heavy conductance modulation. The channel and drift regions with certain resistance can conduct a larger current, giving a small voltage drop. Therefore, in order to analyze the transient operating mechanism at depth, it is of significance to study the potential distribution in the SITH channel in the blocking and conducting states, as well as the variations in the height of the potential barrier in the switching transition process between the blocking and conducting state.

2. Structural description and the transient mechanism of SITH

The channel, cathode, anode and gate regions are doped to $N_{\rm DCH} = 1 \times 10^{14}$ cm^{-3}, $N_{\rm DK} = 1 \times 10^{19}$ cm^{-3}, $N_{\rm AA} = 1 \times 10^{19}$ cm^{-3} and $N_{\rm AG} = 1 \times 10^{19}$ cm^{-3}, respectively. The channel width ($L_{\rm D}$) is 750 μm, the channel length or gate length ($L_{\rm G}$) is 8 μm, the gate-to-gate space (called the channel thickness) is 9 μm, and the repeated period is 25 μm. The drift region between the gate and the anode is an n-type Si single crystal substrate doped with 1×10^{14} cm^{-3} phosphorus. The gate is reversely biased and the anode is forwardly biased when SITH operates normally. The technological processes for fabricating sample devices are not included in this paper because of space restrictions, so please refer to our previous paper[9, 10].

The operating state of SITH is controlled by the height of the potential barrier in the channel. The device works in the blocking state when the potential barrier is high; and in the conducting state when it is low. The device switches from the blocking state to the conducting state when the potential barrier turns from a high level to a low level, and vice versa. The height of the potential barrier in the channel can be controlled by changing the negative gate voltage and/or by positive anode voltage through changing the carrier concentrations in the channel, based on the principle of static induction. The holes injected from the anode diffuse and drift to the terminal of the channel, where they are swept towards the potential saddle in the channel and then obstructed by the reverse electric field directed from the cathode to the saddle point. At the same time, the electrons injected into the channel drift towards the gate region. The electrons diffused from the cathode to the saddle are swept towards the drift region, and the electric field directing at the gate prevents the electrons from entering the gate region.

The density of holes swept into the channel is essentially constant when the gate voltage is increased. The net charge in the depletion layer consists of the density of ionized impurity charges and that of holes, p. The relationship between gate

* Project supported by the Scientific and Technological Supporting Program of Gansu Province, China (No. 097GKCA052).

† Corresponding author. Email: cjliu2011@lzu.edu.cn

Received 21 October 2011, revised manuscript received 22 November 2011

voltage V_G and the potential barrier height can be expressed as:

$$V_G - \phi_{ch} = \frac{q}{\varepsilon_0 \varepsilon_S} \int_0^l \int_0^l (C + p) dx dx, \qquad (1)$$

where ϕ_{ch} is the height of the potential barrier, l is the channel length, and C is the carrier concentration of ionized impurity charges. The integral term is constant. With the increase in gate voltage, the height of the potential barrier is also increased with the same value. The potential barrier in the channel varies linearly with gate bias voltage under low injection ($p \ll C$). The change in potential is larger than that in gate voltage under high injection, and this is the reason why the gate voltage can sensitively control the operating states of SITHs.

The height of the potential barrier in the channel can also be controlled by anode voltage V_A. For the given gate voltage, with the variation in V_A, the anode and cathode currents vary, resulting in the change in carrier density flowing through the channel. This situation changes the net space charge distribution, causing a change in the electric field and potential barrier. The net charge density in the channel is now composed of electrons, n, injected from the cathode, holes, p, swept from the drift region, and ionized impurity charges. A functional relation among these parameters can be written as:

$$\phi_{ch} - V_K = \frac{q}{\varepsilon_0 \varepsilon_S} \int_0^l \int_0^l (C + p - n) dx dx, \qquad (2)$$

where V_K is the cathode voltage. Generally, as the cathode is biased to zero, the change in anode voltage will bring a variation in the height of the potential barrier in the channel. Only a large change in anode voltage, V_A, can give rise to a variation in the carrier density in the channel. In other words, a large variation in anode voltage can bring a relatively small change in the potential barrier in the channel. The variation in height of the potential barrier caused by a small change in gate voltage can only be generated by a relatively large change in anode voltage. The control efficiency of gate voltage, defined as the blocking voltage resulted by the unit gate voltage, is much higher than that of the anode voltage. A small variation in gate voltage can block a very high anode voltage.

3. Dependence of the working state on potential distribution

The working state of the SITH, either in conducting or blocking, is determined by the height of the potential barrier in the channel. The holes injected from the anode are collected by the gate and distributed in the space charge region of the gate, giving rise to a variation in potential distribution. The distribution of holes in the space charge region of the gate is equivalent to an increase in the doping concentration of the gate region. The increase in voltage drop in the space charge region resulting from the Kirk effect in this region is equal to a reduction in the effect of gate voltage on the height of the potential barrier. This is the reason why the SITH switches from the blocking to the conducting state, exhibiting snapback phenomena and negative resistance.

The potential distribution in the SITH channel in the blocking and conducting states is illustrated in Fig. 1. In the blocking state, the potential drops mainly across the depletion region in

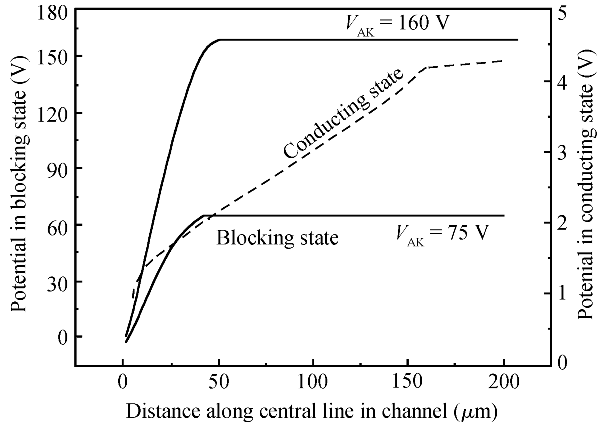

Fig. 1. Comparison of potential distributions in the SITH channel in the blocking and conducting states.

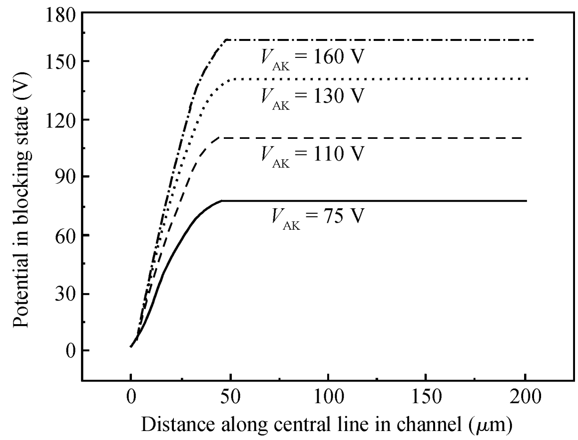

Fig. 2. Potential distribution along the central line of the channel in the blocking state.

the channel, whereas the potential drops chiefly across both the channel and the drift region in the conducting state.

In the blocking state, the space charge region with low carrier concentration in the channel can withstand very high anode voltage. The channel with rather low resistance can transmit large current due to conductance modulation occurring in the channel in the conducting state.

3.1. Potential distribution in the blocking state

The potential distribution along the central lines of the channel in the blocking state is demonstrated in Fig. 2. The space charge region in the channel undertakes all the potential in the blocking state. The potential mainly falls across the channel under low anode bias, with almost no potential dropping across the drift region. But for the large anode voltage, the drift region takes on a part of the potential drop.

Electrical neutrality is kept in the channel when the SITH operates. In high-level injection, the electrical conductance modulation effect occurs in the drift region in which there is no potential barrier, which is equivalent to a resistance. The anode current density is uniform throughout the drift region. The voltage drop across the drift region is directly proportional to the anode current flowing through it. The resistance of the drift region is dependent on the carrier concentration of it. With a low biased voltage, the density of holes injected from the anode is very low, and the electron density is equal to the concentration of ionized impurities. The resistance of the drift region can be written as:

$$R = \int_0^{L_b} \frac{1}{q\mu_n CA} dl = \frac{L_b}{q\mu_n CA}, \tag{3}$$

where L_b is the width of the drift region and A is the area of the device. The resistance, R, is a constant under low injection. According to the high density of carriers and the complicated distribution under high level injection, combined with the transfer function of semiconductor and Ohmic law, the resistance can be expressed as:

$$\begin{aligned} R &= \int_0^{L_b} \frac{1}{q(\mu_n + \mu_p) Ap} dx \\ &= \frac{L_b}{q(\mu_n + \mu_p) A\sqrt{C_1 C_2}} \\ &\times \left[-\arctan \frac{C_1}{\sqrt{C_1 C_2}} + \arctan \frac{C_1 \exp(L_b/l)}{\sqrt{C_1 C_2}} \right], \end{aligned} \tag{4}$$

where C_1 and C_2 are coefficients, which can be written as:

$$C_1 = -N_A \exp\left[-\frac{q(V_{Abi} - V_A)}{kT}\right] \frac{\exp\left(-\dfrac{L_b}{L_p}\right)}{\exp\dfrac{L_b}{L_p} - \exp\left(-\dfrac{L_b}{L_p}\right)}, \tag{5}$$

$$C_2 = N_A \exp\left[-\frac{q(V_{Abi} - V_A)}{kT}\right] \frac{\exp\dfrac{L_b}{L_p}}{\exp\dfrac{L_b}{L_p} - \exp\left(-\dfrac{L_b}{L_p}\right)}. \tag{6}$$

Equation (4) can be reduced with the Taylor series:

$$\begin{aligned} R &= \frac{L_b(\exp(L_b/l) - 1)}{q(\mu_n + \mu_p) AC_2} + \frac{L_b(\exp(L_b/l) - 1)C_1}{3q(\mu_n + \mu_p) AC_2^2} \\ &+ 0\left(\frac{C_1}{C_2}\right)^3. \end{aligned} \tag{7}$$

The concentration of carriers under high level injection can be computed semi-quantitatively:

$$\overline{p}, \overline{n} = m \exp\left(-\frac{q(V_{Abi} - V_A)}{kT}\right), \tag{8}$$

$$\begin{aligned} R &= \int_0^{L_b} \frac{1}{q(\mu_n + \mu_p) AC \exp\left(-\dfrac{q(V_{Abi} - V_A)}{kT}\right)} dx \\ &= \frac{L_b}{q(\mu_n + \mu_p) Am} \exp\frac{q(V_{Abi} - V_A)}{kT}, \end{aligned} \tag{9}$$

where V_{Abi} is the built-in potential of the anode p–n junction, and m is a coefficient. So, the voltage falls across the drift region for low and high current are given by Eqs. (10) and (11), respectively.

$$V_{\text{drift, L}} = I_A R_{\text{drift}} = \frac{I_{A0} L_b}{q\mu_n CA} \exp\left(-\frac{q(V_{Abi} - V_A)}{kT}\right), \tag{10}$$

$$V_{\text{drift, H}} = IR_{\text{drift}} = \frac{I_{A0} L_b}{q(\mu_n + \mu_p) AC}. \tag{11}$$

With the increase in anode biased voltage, the increase in voltage drop across the drift region becomes small. The voltage is considered to have fallen across the space charge region of the gate. With the increase in positive anode voltage, the space charge region of the reversely biased pn junction between the gate and drift region widens. The width of the space charge region is determined by the net charge density and applied voltage. The electron concentration in the space charge region is very low, and can be ignored. Taking into account the ignorable concentration of holes in the space charge region for high anode bias, the equation describing the dependence of voltage drop across the space charge region on net space charge and width can be expressed as:

$$V = \frac{q}{\varepsilon} \int_0^{L_G} \int_0^{L_G} (C + p)\, dx dx. \tag{12}$$

Taking the carrier concentration to be constant in the space charge region and the higher doping concentration of the gate than that in drift region into account, Equation. (12) can be reduced to:

$$V = \frac{q(C + \overline{p})}{2\varepsilon} L_G^2. \tag{13}$$

For a low density of holes, the voltage drop across the space charge region is expressed as:

$$V = \frac{qC}{2\varepsilon} L_G^2. \tag{14}$$

The potential distribution in the gate junction is influenced by the high concentration of holes. The width of the space charge region can be obtained based on the above analysis:

$$L = \sqrt{\frac{2\varepsilon V}{q(C + \overline{p})}}. \tag{15}$$

A large concentration of holes injected by a high forwardly biased anode voltage increases the positive charge in the space charge region, this being equal to an increase in doping concentration and a decrease in the width of the space charge region. Both the effects of anode voltage and the high concentration of holes keep the space charge region of the gate from changing, as shown in Fig. 3.

3.2. Potential distribution in the conducting state

A heavy conductance modulation effect occurs in the channel in the conducting state. The drift region with a high concentration of carriers cannot bear high voltage. Due to conductance modulation, almost no net space charge exists in the channel region. Therefore, there is no electric field. The high concentration of carriers in the channel due to conductance modulation

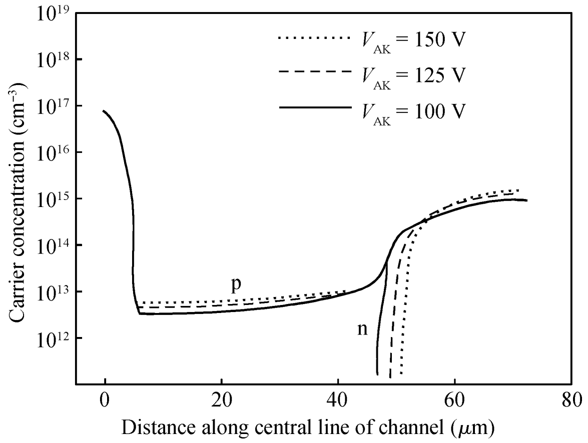

Fig. 3. Carrier distribution in the channel under high anode bias.

results in a very low resistance and a small voltage drop. The heavy conductance modulation both in the channel and drift regions is equivalent to a series of two resistors. The ohmic voltage drop across the drift region can be expressed as:

$$V = I\int_0^{L_b}\frac{1}{q\left(\mu_n+\mu_p\right)Ap}\mathrm{d}x. \tag{16}$$

The resistance of the channel is given by:

$$R = \int_l \frac{W_{\text{eff}}qp\mu_n\mu_p}{\mu_n+\mu_p}\mathrm{d}l, \tag{17}$$

where W_{eff} is the effective width of the channel. The voltage drop across the channel is written as:

$$V = I_R = I_K\int_l \frac{W_{\text{eff}}qp\mu_n\mu_p}{\mu_n+\mu_p}\mathrm{d}l. \tag{18}$$

The space charge region of the pn junction between the gate and channel shrinks because of a large account of holes existed, and a conducting channel is formed, as indicated in Fig. 4. The resistance along the central line of the channel is the series of drift region and channel resistances, which determine the voltage drop in the conducting state.

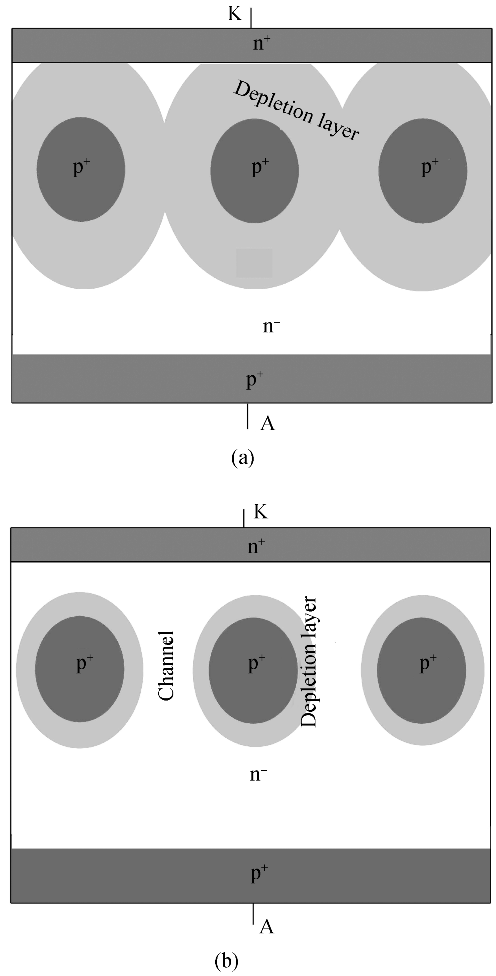

Fig. 4. Distribution of space charge region (a) in the blocking state and (b) in the conducting state.

4. *I–V* characteristics

The simulated and experimentally measured *I–V* characteristics of the SITH are illustrated in Fig. 5. The maximum leakage current is less than 0.1 A/cm in the blocking state. The current is higher than 1 A/cm with a very low voltage drop in the conducting state, with a leakage current of about 10 times, indicating typical switching-on and switching-off states.

4.1. *I–V* characteristics in the conducting state

For the different gate voltages, the change in blocking voltage V_{block} is large. With a rise in V_{GK}, V_{block} rises much higher in a nonlinearly manner. The current at the turn-around point is almost the same. However, with the increase in gate voltage, V_{GK}, the turn-around current increases slightly, indicating that there are more holes injected from the anode, which is consistent with the results of Eq. (18). The density of current at the turn-around point reflects the concentration of holes injected from the anode region. There are more holes injected from the anode and more electrons swept into the channel for the high density of current. The increase in the concentration of holes in the space charge region of the gate gives rise to an increase in the voltage drop of V_{GK} across the space charge region of the gate, gradually reducing the influence of gate bias on the potential barrier in the channel. Once the effect of gate voltage on the potential barrier vanishes, the device converts from off-state to on-state. The anode current, I_A, independent of gate voltage due to the Kirk effect, increases rapidly with the increase in V_A in the conducting state, in an almost upright fashion.

4.2. *I–V* characteristics in the blocking state

The anode current, I_A, increases with V_A in different ways in the blocking state. According to Eq. (12), in the low anode current region, I_A is the generation current and increases slowly, as indicated by the curves in section 1 of Fig. 6. The variation in I_A with V_A is relatively small, and the logistic of anode current is linear with anode bias voltage. In other words, the I_A current increases with V_A exponentially in the high current region. For the large gate voltage, the variation in I_A be-

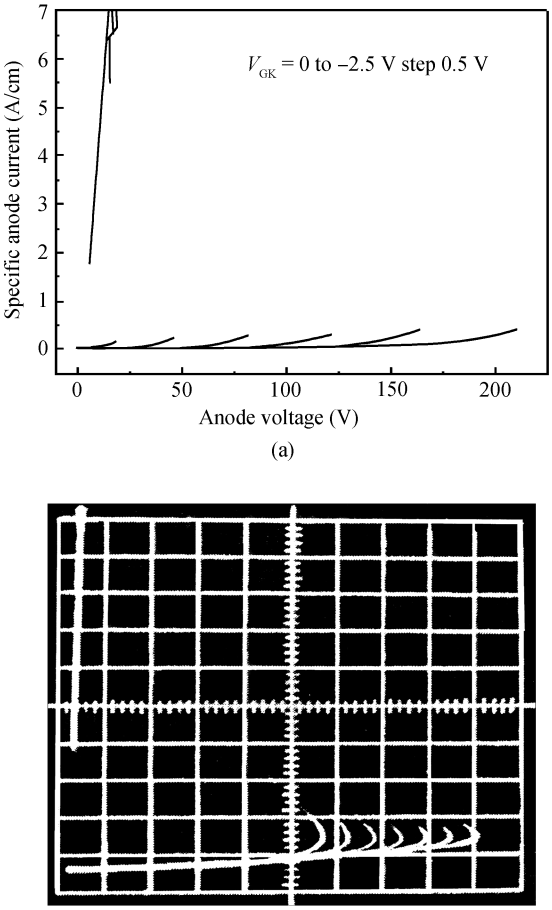

Fig. 5. I–V characteristics of the SITH: (a) simulated and (b) measured.

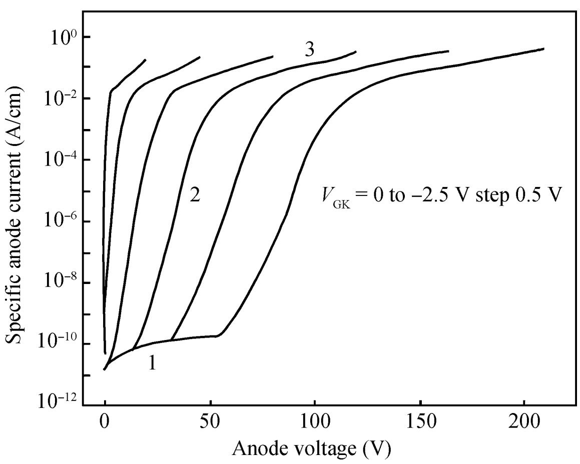

Fig. 6. I–V characteristics of the SITH in the blocking state.

comes small (it changes by less than two orders). A small variation in gate voltage may cause a change in I_A of many orders, even though the anode voltage V_A remains constant, as shown in Section 2 of Fig. 6.

The current is almost constant in the changing region of every section. The blocking state zone can be defined according to the current magnitude. SITHs operate in the generation current region when I_A is less than the maximum of the generation current that can be expressed as:

$$I = \int_{\sigma_G} G \mathrm{d}\sigma_G, \tag{19}$$

where σ_G is the area of the depletion layer of the gate, and G is the generation rate. The drift region is completely depleted. When the I_A anode current is higher than a critical value, the SITH works in the high current region. The variation in I_A with V_A is relatively small, and the current increases exponentially in the medium section.

5. Conclusions

In order to raise the blocking voltage, it is necessary to increase the length of the drift region. But a drift region that is too long may cause the conducting voltage drop to deteriorate. A wide channel area can improve the current density in the conducting state, but gives rise to an increase in the leakage current in the blocking state. Although high doping concentrations in the anode and cathode regions raise the current density, they also raise the heights of the potential barriers at the anode and cathode in the conducting state, increasing power consumption. Though highly doped substrates help raise the doping concentration of the device, the width of the space charge region in the channel is reduced, resulting in deterioration of the voltage-resistant capability and switching speed of the device.

An optimum compromise among all these factors and parameters is summarized as follows: the effective width of the channel is 1.5 μm besides the depletion layer and gate body, the length of the drift region is 150 μm, the distance of the saddle point from the end of the channel near the cathode is 5 μm, and the doping concentration of the substrate, anode and cathode is 1×10^{14}, 1×10^{19} and 1×10^{19} cm^{-3}, respectively.

The results reported in this paper provide a useful guide to avoiding blindness, to a certain extent, when designing and fabricating SITHs. The mutual constraint relationship among the potential distribution, I–V characteristics, transient performance, and parameters such as materials, geometrical structure and technological processing has been revealed for the first time.

References

[1] Wang Y S, Wu R, Liu C J, et al. Improvement on high current performance of static induction transistor. Chinese Journal of Semiconductors, 2007, 28(8): 12

[2] Wang Y S, Li H R, Wu R, et al. Mechanism of reverse snapback on I–V characteristics of power SITHs with buried gate structure. Journal of Semiconductors, 2008, 29(3): 461

[3] Wang Y S, Li H R, Wang Z T, et al. Improvements on high voltage performance of power static induction transistors. Journal of Semiconductors, 2009, 30(10): 104003

[4] Nishizawa J I, Motoya K, Itoh A. The 2.45 GHz 36 W CW Si recessed gate type SIT with high gain and high voltage operation. IEEE Trans Electron Devices, 2000, 47: 482

[5] Sung Y M, Casady J B, Dufrene J B, et al. A review of SiC static induction transistor development for high-frequency power amplifiers. Solid-State Electron, 2002, 46: 605

[6] Nishizawa J I, Terasaki T, Shibata J. Field-effect transistor versus analog transistor (static induction transistor). IEEE Trans Electron Devices, 1975, 22(4): 185
[7] Nishizawa J I, Ohmi T, Chen H. Analysis of static characteristics of a BSIT. IEEE Trans Electron Devices, 1982, 29: 1233
[8] Nishizawa J I, Muraoka K, Tamamushi T, et al. Low-loss high-speed switching devices: 2300-V 150-A static induction thyristor. IEEE Trans Electron Devices, 1985, 32: 822
[9] Wang Y S, Wu R, Liu C J, et al. Researches on the injected charge potential barrier occurring in the static induction transistor in the high current region. Semicond Sci Technol, 2008, 23: 152
[10] Wang Y S, Luo X L, Li H R, et al. Improvements on radiation-hardened performance of static induction transistor. Science China: Information Sciences, 2010, 53(5): 1089